Targeting Treg-Expressed STAT3 Enhances NK-Mediated Surveillance of Metastasis and Improves Therapeutic Response in Pancreatic Adenocarcinoma

Miles Piper[1], Benjamin Van Court[1], Adam Mueller[1], Shuichi Watanabe[1,2], Thomas Bickett[1], Shilpa Bhatia[1], Laurel B. Darragh[1,3], Max Mayeda[1], Diemmy Nguyen[1], Jacob Gadwa[1], Michael Knitz[1], Sophia Corbo[1], Rustain Morgan[4], Jung-Jae Lee[5], Alexander Dent[6], Karyn Goodman[1,7], Wells Messersmith[8], Richard Schulick[2,3], Marco Del Chiaro[2], Yuwen Zhu[3], Ross M. Kedl[3], Laurel Lenz[3], and Sana D. Karam[1]

ABSTRACT

Purpose: Metastasis remains a major hurdle in treating aggressive malignancies such as pancreatic ductal adenocarcinoma (PDAC). Improving response to treatment, therefore, requires a more detailed characterization of the cellular populations involved in controlling metastatic burden.

Experimental Design: PDAC patient tissue samples were subjected to RNA sequencing analysis to identify changes in immune infiltration following radiotherapy. Genetically engineered mouse strains in combination with orthotopic tumor models of PDAC were used to characterize disease progression. Flow cytometry was used to analyze tumor infiltrating, circulating, and nodal immune populations.

Results: We demonstrate that although radiotherapy increases the infiltration and activation of dendritic cells (DC), it also increases the infiltration of regulatory T cells (Treg) while failing to recruit natural killer (NK) and CD8 T cells in PDAC patient tissue samples. In murine orthotopic tumor models, we show that genetic and pharmacologic depletion of Tregs and NK cells enhances and attenuates response to radiotherapy, respectively. We further demonstrate that targeted inhibition of STAT3 on Tregs results in improved control of local and distant disease progression and enhanced NK-mediated immunosurveillance of metastasis. Moreover, combination treatment of STAT3 antisense oligonucleotide (ASO) and radiotherapy invigorated systemic immune activation and conferred a survival advantage in orthotopic and metastatic tumor models. Finally, we show the response to STAT3 ASO + radiotherapy treatment is dependent on NK and DC subsets.

Conclusions: Our results suggest targeting Treg-mediated immunosuppression is a critical step in mediating a response to treatment, and identifying NK cells as not only a prognostic marker of improved survival, but also as an effector population that functions to combat metastasis.

Introduction

Despite advances in treatment modalities, pancreatic ductal adenocarcinoma (PDAC) remains one of the worlds' deadliest malignancies with a dismal 5-year overall survival rate of 9% (1). The primary obstacle in treating PDAC remains the disease's aggressiveness and preponderance to metastasize (2). Current evidence suggests that metastasis is a complex process involving multiple cellular populations and various signaling pathways, making it difficult to target effectively (3). Not only this, PDAC has been shown to exhibit distinct molecular behaviors, making it resistant to conventional and targeted therapies (4). This treatment failure has been attributed to multiple inherent and adaptive biological origins, perhaps one of the most significant being the resistance resulting from an immunosuppressive tumor microenvironment (TME).

The TME of PDAC is frequently characterized as an immune "desert"; one that is devoid of cytotoxic effector immune cells such as natural killer (NK), CD4, and CD8 T cells, and permeated by highly immunosuppressive cells such as regulatory T cells (Treg; ref. 5–8). Various immune modulating agents, including radiotherapy, have been used to invigorate an immune response in PDAC. However, these modalities have been met with limited efficacy. A recent clinical trial (9) showed that the addition of stereotactic radiotherapy (SBRT), a therapy known to invigorate an immune response, was inferior to the standard care with worsened disease-free survival outcomes, leading to early closure of the trial. While technical delivery of the therapy and radiation dose continue to be debated (10, 11), what remains unknown are the cellular and molecular mechanisms of how SBRT affects immunosurveillance properties within the PDAC TME that contribute not only to local growth, but also to metastatic dissemination in this disease. Using patient specimens before and after SBRT treatment, we identified Tregs, NK cells, and dendritic cells (DC) as key immune cells mediating response to radiotherapy. Within these cell types, we also identified the transcription factor STAT3 as an over-expressed signal within the NK and Treg immune cell subsets. STAT3 is known to be activated in PDAC; its expression correlates with tumor grade (12),

[1]Department of Radiation Oncology, University of Colorado, Anschutz Medical Campus, Aurora, Colorado. [2]Department of Surgery, University of Colorado, Anschutz Medical Campus, Aurora, Colorado. [3]Department of Microbiology and Immunology, University of Colorado, Anschutz Medical Campus, Aurora, Colorado. [4]Department of Radiology, University of Colorado, Anschutz Medical Campus, Aurora, Colorado. [5]Department of Chemistry, University of Colorado Denver, Denver, Colorado. [6]Department of Microbiology and Immunology, Indiana University School of Medicine, Indianapolis, Indiana. [7]Department of Radiation Oncology, Mount Sinai Hospital, New York, New York. [8]Department of Medical Oncology, University of Colorado, Anschutz Medical Campus, Aurora, Colorado.

Note: Supplementary data for this article are available at Clinical Cancer Research Online (http://clincancerres.aacrjournals.org/).

Corresponding Author: Sana D. Karam, Department of Radiation Oncology, University of Colorado Denver, 1665 Aurora Court, Aurora, CO 80045. Phone: 720-848-0910; Fax: 720-848-0238; E-mail: sana.karam@cuanschutz.edu

Clin Cancer Res 2022;28:1013–26

doi: 10.1158/1078-0432.CCR-21-2767

Translational Relevance

The inherent challenges in treating pancreatic ductal adenocarcinoma (PDAC) arise, in part, from an adaptive biological resistance resulting from an immunosuppressive tumor microenvironment (TME). Although stereotactic body radiotherapy (SBRT) has been used in PDAC treatment as a means of invigorating a local immune response, we demonstrate in a paired analysis of patient tissue samples that despite enhancing antigen presentation via increased dendritic cells, SBRT also induces the infiltration of immunosuppressive cells such as regulatory T cells and fails to improve natural killer cell or T-cell effector function, two cell types that correlate with response to therapy. Moreover, while STAT3 is a known critical mediator of disease progression, metastasis, and resistance to therapy in PDAC, its effect on immune subsets within the TME of PDAC remains less characterized. Here, we show that systemic delivery of a STAT3 antisense oligonucleotide in combination with SBRT results in tumor growth regression, decreased metastasis, and reversal of immunosuppression.

and is a driver of therapeutic resistance in different models of PDAC (13, 14). However, the mechanisms by which STAT3 signaling on immune subsets affects their cytotoxic, suppressive, or surveillance potential, and how this regulates local growth and systemic dissemination in the context of radiotherapy remains an unexplored topic.

In the current study, we tested the hypothesis that the sustained activation of STAT3 within the NK and Treg compartments not only hinders the antitumor potency of SBRT, but promotes metastasis and disease spread in PDAC. Observing that pharmacologic and genetic depletion of Tregs and NK cells enhances and attenuates response to SBRT, respectively, we aimed to test their functionality following specific STAT3 inhibition. Using FoxP3-Cre/STAT3 fl and NKp46-Cre/STAT3 fl animal models, we found STAT3 knockout (KO) on Tregs decreases local progression and metastatic spread, and increases DC, NK, and CD4 effector T-cell function. In contrast, knockdown of STAT3 on NK cells accelerated tumor growth and metastasis when combined with radiotherapy. This effect was reversed with Treg depletion, suggesting that targeting Tregs is an essential component to obtaining an immune response as this cell type exerts a negative immunoregulatory function on NK cells and DCs. This was further validated using a STAT3 antisense oligonucleotide (ASO), which showed that simultaneous targeting of NK cells and Tregs results in the activation of CD103 DC and T effector cell functions, as well as decreased tumor growth and metastasis. The data presented here suggest that dual targeting of STAT3 on Tregs and NKs invigorates DC and T effector cell responses, improves response to SBRT, and results in diminished metastatic burden, providing rationale for follow-up studies in patients with PDAC.

Materials and Methods

More detailed materials and methods can be found in the supplemental methods.

Human tissue and trial specimens

Written consent was obtained for all tumor sample collections. Studies were performed in accordance with U.S. Common Rule and approved by institutional review board. Patient archival tumor samples ($n = 16$) were identified and obtained from biorepository and collected per COMIRB13–0315. Patients were selected from all borderline resectable pancreatic cancer patients seen through University of Colorado pancreas multidisciplinary clinic between 1/2013–12/2018 who were treated with either FOLFIRINOX or gemcitabine-based neoadjuvant chemotherapy and stereotactic body radiotherapy (SBRT) administered as 30–33Gy in 5 fractions, followed by surgical resection. Response to treatment was determined by pathologic scoring at the time of surgery at the University of Colorado.

Patient plasma samples ($n = 13$) were collected as part of a Phase I radiation dose-escalation clinical trial (NCT02873598) before, during (6 hours post), and post (6 weeks) SBRT. All patients received neoadjuvant chemotherapy prior to SBRT. SBRT doses ranged from 9Gy × 3 fractions to 11Gy ×3 fractions. Samples were collected and analyzed per COMIRB19–0328.

RNA sequencing/xCell analysis

TempO-Seq FFPE Assay 96 sample kit was used for RNA sequencing (RNA-seq) library preparation (BioSpyder). Formalin-fixed, paraffin-embedded slides of fine needle aspiration biopsy and post-neoadjuvant patient samples were obtained from University of Colorado biorepository. Samples were pooled and run in two sequencing lanes using NextSeq high throughput sequencing instrument (Illumina). Reads were aligned and counts generated using Biospyder TempO-Seq platform. Genes with <1 mean raw counts or <1 mean counts per million were removed from the dataset. TempO-Seq data were corrected for attenuation factors and analyzed using xCell (15) to estimate differences in cell type composition of samples (https://xcell.ucsf.edu/).

Local and metastatic orthotopic *in vivo* models

Female C57BL6 (6 weeks old) were purchased from Jackson Laboratories (Indianapolis, IN). All mice were cared for in accordance with the ethical guidelines and conditions set and overseen by the University of Colorado Anschutz Medical Campus Animal Care and Use Committee. Protocols used for animal studies were reviewed and approved by the Institutional Animal Care and Use committee at the University of Colorado Anschutz Medical Campus.

Local orthotopic implantations were conducted by first anesthetizing mice using isoflurane and making a 1-cm incision in the left subcostal region. Mouse pancreata were located, externalized, and injected with 200,000 KPC cells suspended 1:1 in Matrigel (Corning, NY). Pancreata were then reintroduced into abdomen and mice peritoneum and skin were closed. Protocol described in further detail (16).

Metastatic orthotopic implantations were conducted as above with spleen externalization following subcostal incision. Spleens were first ligated with horizon clips and one hemispleen was injected with 200,000 KPC cells suspended in 50ul 10% RPMI followed by washout injection of 50μl PBS. Splenic vessels were then ligated with horizon clips and hemispleen was excised prior to closure of peritoneum and skin. Metastatic implantation described in further detail (17).

Drug administration

Murine STAT3 ASO (481549–30, Ionis Pharmaceuticals) or control ASO were dosed at 50 mg/kg diluted in sterile saline three times per week, intraperitoneally, starting at one day prior to radiotherapy and maintained for the duration of the study. Diphtheria toxin (DT) was dosed at 50 μg twice per week beginning one day prior to tumor implantation. αNK1.1 antibody was administered at a dose of 200 μg twice per week beginning one day prior to implantation.

Results

Radiotherapy increases infiltration and activation of DCs but fails to activate NK and CD8 T-cell responses in patients with PDAC

To understand the changes to the immune landscape mediated by SBRT in pancreatic cancer, we performed paired RNA-seq and cell type composition analysis (15) on human PDAC tumors pre- and post-treatment with SBRT. While our results showed a decrease in overall immune infiltration (**Fig. 1A**), there were significant changes in specific immune subsets. Although DC frequency and activation were significantly increased after SBRT (**Fig. 1B**), there was an increase in immunosuppressive Tregs (**Fig. 1C**), and no change in CD8 T-cell infiltration post-SBRT (**Fig. 1D**). NK-cell infiltration was notably reduced following SBRT (**Fig. 1E**), a finding of clinical relevance given the correlation we observed between NK cells and improved disease-free survival (**Fig. 2A**).

To examine potential biomarkers of response, we next focused our analysis on responders and nonresponders to SBRT as defined by pathologic response at the time of surgery. Using xCell sequencing analysis (15), three immune populations were identified as effective in predicting response to SBRT: NK cells, CD8 effector memory T cells, and naïve CD8 T cells. Through this analysis, we found significantly more NK cells were present in the tumors of patients that responded to SBRT at baseline (**Fig. 1F**). In addition, responders had significantly fewer naïve CD8 T cells and significantly more CD8 effector memory T cells in the TME prior to receiving treatment (**Fig. 1F**), suggesting an important balance of NK and CD8 T-cell activation in mediating response to radiotherapy in PDAC.

We next sought to understand the systemic effects of radiotherapy by analyzing the cytokines present in the peripheral blood of patients with PDAC before, during, and after SBRT. We observed no changes in the immunostimulatory cytokines IL2, IL12, IFNγ, and TNFα with radiotherapy, further validating the claim that SBRT alone is insufficient in eliciting a durable, T-cell–mediated antitumor immune response. However, this analysis revealed that IL15, an important mediator of NK-cell activation (18), was markedly reduced post-SBRT (**Fig. 1G**). Together, these data suggest that while radiotherapy is capable of recruiting and activating DCs, it is insufficient in overcoming the resulting immunosuppression and fails to activate the cytotoxic populations of NK and CD8 T cells.

Tregs and NK cells express pSTAT3 in the TME of pancreatic cancer

Having identified Tregs and NK cells as pertinent immune cells in the response to radiotherapy, we next sought to understand their mechanisms of action in the TME of PDAC. As STAT3 is an important mediator of effector function in a variety of immune subpopulations including NK cells, Tregs, and myeloid cells (19–21), we began by determining its expression pattern at baseline in human samples. Using multiplexed IHC, we found that pancreatic tumors were largely acellular, as shown by cytokeratin expression, with sparse infiltration of CD4 and CD8 T cells (**Fig. 1H**). This analysis also showed that pSTAT3 commonly co-stained with CD56, suggesting frequent STAT3 activation in NK cells (Supplementary Fig. S2A and S2B). Moreover, although Treg abundance was low at baseline, we found that pSTAT3 colocalized with FoxP3$^+$ cells (Supplementary Fig. S2A and S2B). Further, using a flow cytometry–based analysis on murine tumors, we observed a significant increase in pSTAT3 expression in intratumoral FoxP3$^+$ and a trend toward increased pSTAT3 expression in intratumoral NKp46$^+$ populations following radiotherapy in orthotopically implanted PK5L1940 pancreatic tumors (**Fig. 1I**). Taken together, these data are both consistent with previous characterizations of the TME of PDAC and are suggestive of a role for STAT3 in the functional capacity of NK cells and Tregs following radiotherapy.

Genetic and pharmacologic targeting of Tregs or NKs results in altered responses to radiotherapy treatment

Given our patient sequencing data and multiplexed IHC staining identifying Tregs and NK cells as relevant intratumoral populations to the immune response following radiotherapy, we next hypothesized that depletion of these two populations would have significant effects on the therapeutic efficacy of radiotherapy. Due to the suppressive nature of Tregs, as well as The Cancer Genome Atlas (TCGA) analysis showing a correlation between disease-free survival and low Treg infiltration in PDAC (**Fig. 2B**), we hypothesized that Treg depletion would improve response to radiotherapy. To test this hypothesis, we selectively depleted Tregs using both an αCD25 Treg-depleting antibody and the DEpletion of REGulatory T cells (DEREG) mouse model (22) wherein FoxP3-expressing Tregs can be selectively depleted through administration of DT. Using a local orthotopic tumor model (23), we found that pharmacologic depletion of Tregs significantly improved survival when treated with radiotherapy (**Fig. 2C**). Similarly, and validating Tregs as a therapeutic target in combination with radiotherapy, genetic depletion of Tregs in the DEREG model led to a significant improvement in overall survival in response to radiotherapy (**Fig. 2D**).

Further, due to our clinical data highlighting the importance of NK cells in the prognosis of patients with PDAC, we next postulated that depletion of NK cells would attenuate response to radiotherapy. Using antibody-mediated depletion, we found that the response to radiotherapy was significantly reduced in the absence of NK cells (**Fig. 2E** and **F**), consistent with our human data that showed a lack of IL15 production and NK activation post-radiation. In addition, mice treated with NK-cell depletion and radiotherapy were also found to have increased circulating tumor cells (CTC) over their radiotherapy only controls (**Fig. 2G**), suggesting an important role for NKs in controlling metastatic burden.

Targeting Treg-expressed STAT3 results in enhanced control of local and distant disease progression

Given our observed increase in Tregs after radiotherapy, and previous studies implicating Treg-expressed STAT3 in several immunosuppressive pathways (20, 24), we next hypothesized that inhibition of STAT3 in Treg cells would improve response to radiotherapy and overcome radiation-induced immunosuppression. To test this hypothesis, we utilized the FoxP3-Cre/STAT3 fl mouse model wherein STAT3 is genetically knocked out in FoxP3-expressing cells. Using a metastatic tumor model in which PK5L1940 PDAC tumor cells are injected through splenic vessels and reproducibly form metastatic lesions in the liver (17), we found that STAT3 KO of FoxP3$^+$ cells resulted in significantly improved survival (MS = 32.5 days) over control (MS = 23.5 days), which was further improved with radiotherapy treatment (MS = 37 days; **Fig. 3A**). We found a similar trend in a local orthotopic tumor model wherein survival was improved upon STAT3 KO of Tregs in combination with radiotherapy (Supplementary Fig. 3A). Together, these data illustrate a role for Treg-expressed STAT3 in promoting not only local, but also distant disease progression.

Inhibiting STAT3 on Tregs results in enhanced activation of circulating and infiltrating immune populations

We next sought to understand what changes in immune populations were mediating this improved response to radiotherapy following STAT3 KO of FoxP3^{+} cells. Using a flow cytometric analysis (representative flow plots in Supplementary Fig. 1), we found significantly increased activation of intratumoral CD4 T cells following radiotherapy in FoxP3-Cre/STAT3 fl mice (**Fig. 3B**). Similarly, circulating CD4 T cells in the blood of FoxP3-Cre/STAT3 fl mice treated with radiotherapy had an increase in the expression of the activation markers CD44 and IFNγ over radiotherapy alone and, importantly, a decrease in IL10 expression over radiotherapy and STAT3 KO alone (**Fig. 3C**), suggesting a robust, systemic activation of a CD4 T-cell response. Of note, we found STAT3-deficient Tregs had significantly reduced FoxP3 expression compared with wild-type (WT) Tregs (Supplementary Fig. 3B). Further, CD8 T cells and NK cells, two directly cytotoxic populations, showed increased expression of the activation markers CD44 and NKG2D, respectively, in the circulating blood of FoxP3-Cre/STAT3 fl mice treated with radiotherapy over radiotherapy alone (**Fig. 3D**). This analysis also revealed that DCs in the draining lymph nodes of FoxP3-Cre/STAT3 mice treated with radiotherapy expressed the highest level of the activation marker CD80 (**Fig. 3E**), suggesting a higher functional capacity for nodal DCs when STAT3 signaling is inhibited in Tregs. To further substantiate these

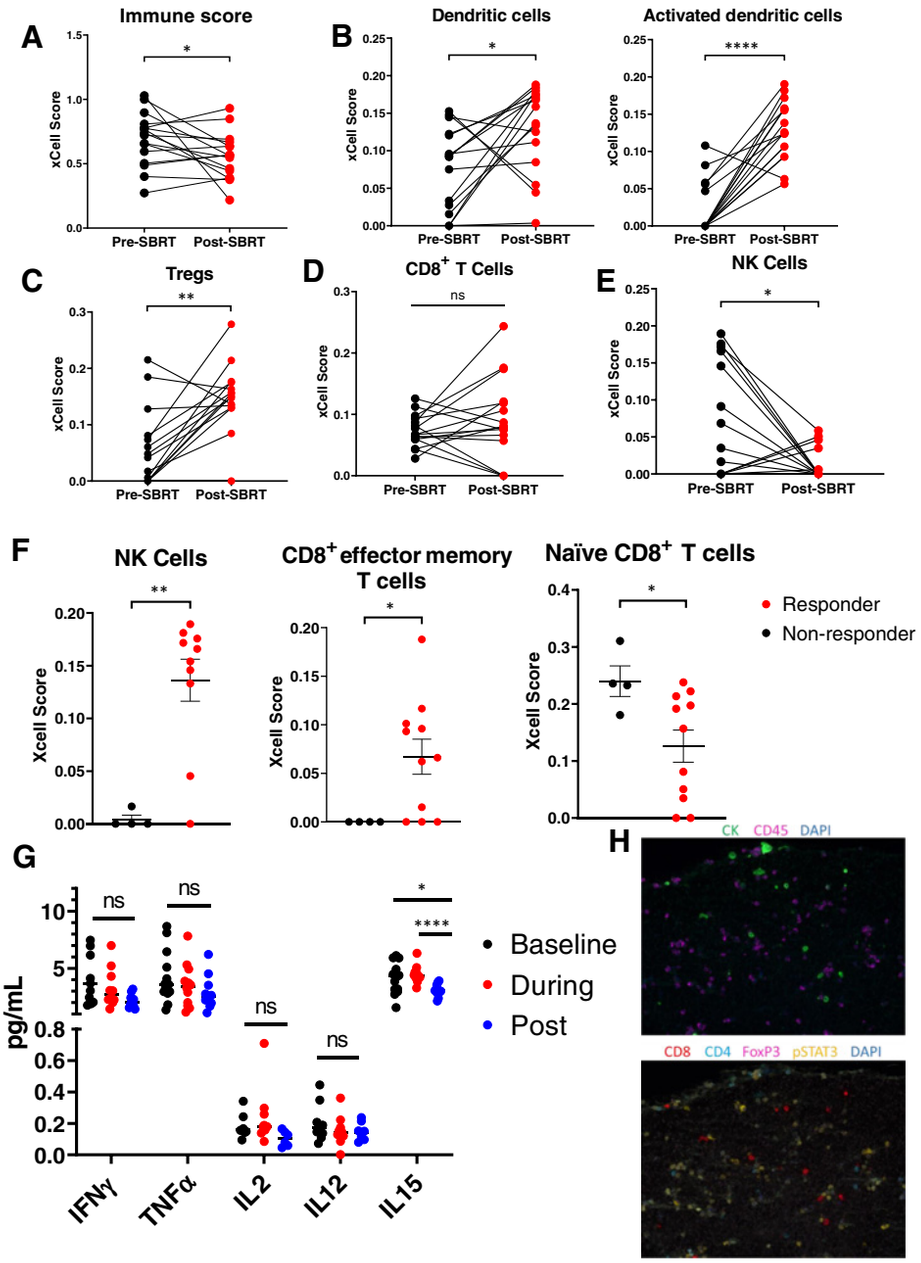

Figure 1.

SBRT increases intratumoral dendritic cell activation and Treg frequency, fails to activate effector T/NK cells. Paired RNA-seq of human PDAC tumors ($n = 16$) before and after treatment with SBRT showing changes in overall immune infiltration (**A**), as well as changes in the frequency (left) and activation (right) of DCs (**B**), Tregs (**C**), CD8 T cells (**D**), and NK cells (**E**). **F,** Difference between NK cells (left), CD8 effector memory T cells (center), and naïve CD8 T cells (right) in responders ($n = 10$) and nonresponders ($n = 4$). Data generated using xCell cell type enrichment analysis, relative expression shown as xCell Score. **G,** Mesoscale chemokine analysis of patient PDAC serum samples ($n \geq 9$) before, during (6 hours post), and post (6 weeks) radiotherapy for IL2, IL12, IFNγ, TNFα, and IL15. Concentrations given in pg/mL. Error bars represent SEM. *P* values calculated with Students *t* test. *, $P < 0.05$; ****, $P < 0.0001$. **H,** Representative images showing overall tumor cellularity and relative immune infiltration in human biopsy PDAC samples. Top, CD45 (magenta) and CK19 (green) expression; bottom, stained for immune subset and activation markers including CD8 (red), CD4 (cyan), FoxP3 (magenta), and pSTAT3 (yellow). Images are different regions from the same slide as in Supplementary Fig. S2D. All slides cut at 4 μm. (*Continued on the following page.*)

Figure 1.
(*Continued.*) **I,** Flow cytometric analysis of murine tumors showing pSTAT3 MFI in tumor-infiltrating FoxP3$^+$ (left) and NKp46$^+$ (right) cells ($n \geq 3$ per group).

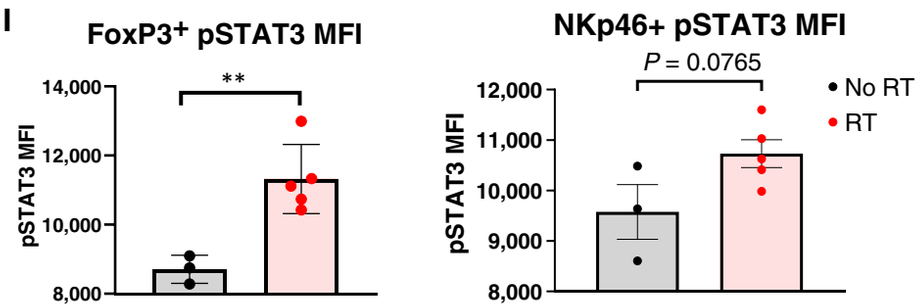

data, we performed multiplexed cytokine analysis on the serum of tumor-bearing mice and found that STAT3 KO on FoxP3$^+$ cells in combination with radiotherapy results in a relative increase in available IL2 and IL1β, two important mediators of T-cell activation. Further, this analysis showed relative decreases in circulating IL4, IL10, and IL13 levels in combination-treated mice, three cytokines involved in promoting systemic immunosuppression. Importantly, combination-treated mice also had an increase in IL15 production over KO alone (**Fig. 3F**). These data, along with the effect data, are suggestive of enhanced immune activation, particularly of NK cells, following STAT3 KO of FoxP3$^+$ cells combined with radiotherapy.

Figure 2.
Low levels of Tregs, high levels of NK cells correlate with survival in PDAC. TCGA disease-free survival analysis of patients stratified by levels of NK cells (**A**) and Tregs (**B**). **C,** Kaplan–Meier survival analysis of WT C57BL/6 mice implanted with local orthotopic pancreatic tumors and treated with radiotherapy (RT) and αCD25 Treg-depleting antibody ($n \geq 6$ mice per group). **D,** Kaplan–Meier survival analysis of WT C57BL/6 and DEREG mice treated with and without RT ($n \geq 5$ mice per group). **E,** Kaplan–Meier survival analysis of WT C57BL/6 mice implanted with local orthotopic pancreatic tumors and treated with RT and αNK1.1 NK-cell–depleting antibody ($n \geq 8$ mice per group). **F,** Kaplan–Meier survival analysis of WT C57BL/6 mice implanted with orthotopic tumors treated with or without RT and with or without αNK1.1 antibody ($n = 8$ per group). *P* values calculated by Mantel–Cox test. **G,** Quantification of CTCs (defined as CD45$^-$/EpCAM$^+$) in the blood of tumor-bearing C57BL/6 mice treated with RT and with or without αNK1.1 NK-cell–depleting antibody ($n \geq 6$ per group). *, $P < 0.05$; **, $P < 0.01$; ***, $P < 0.001$.

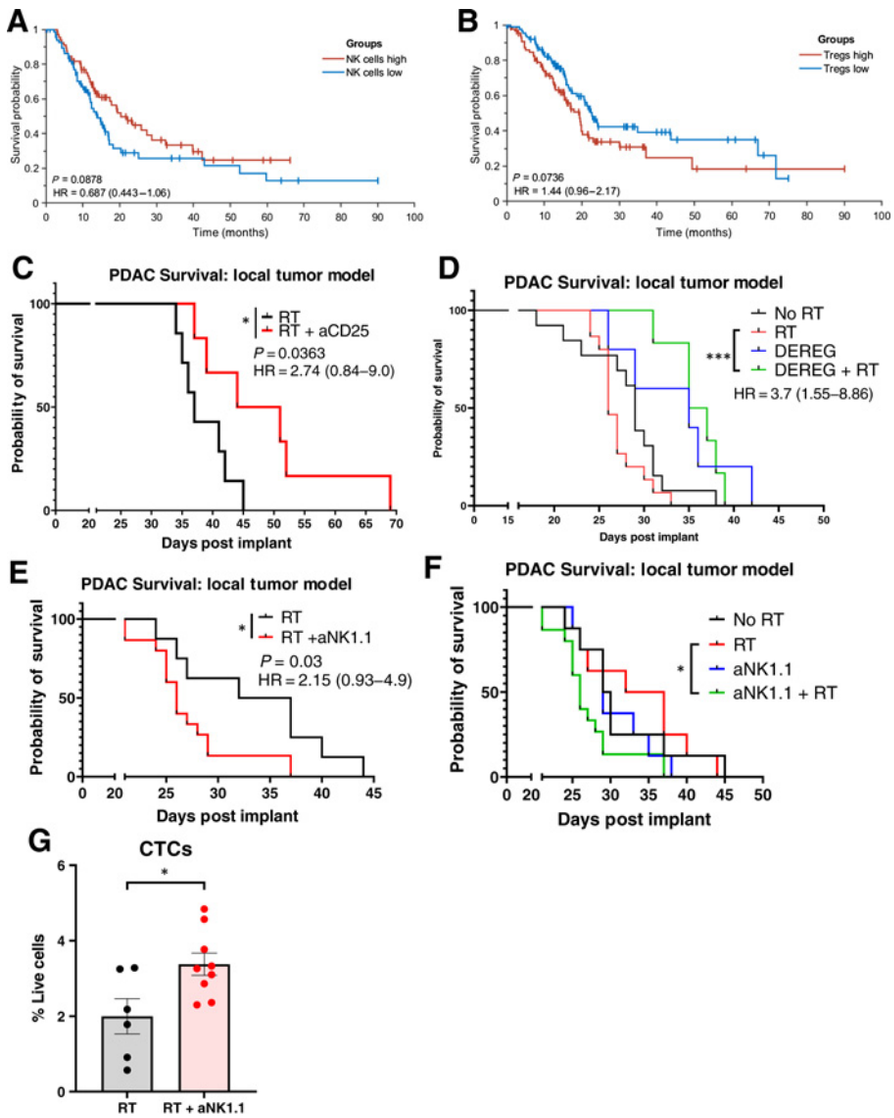

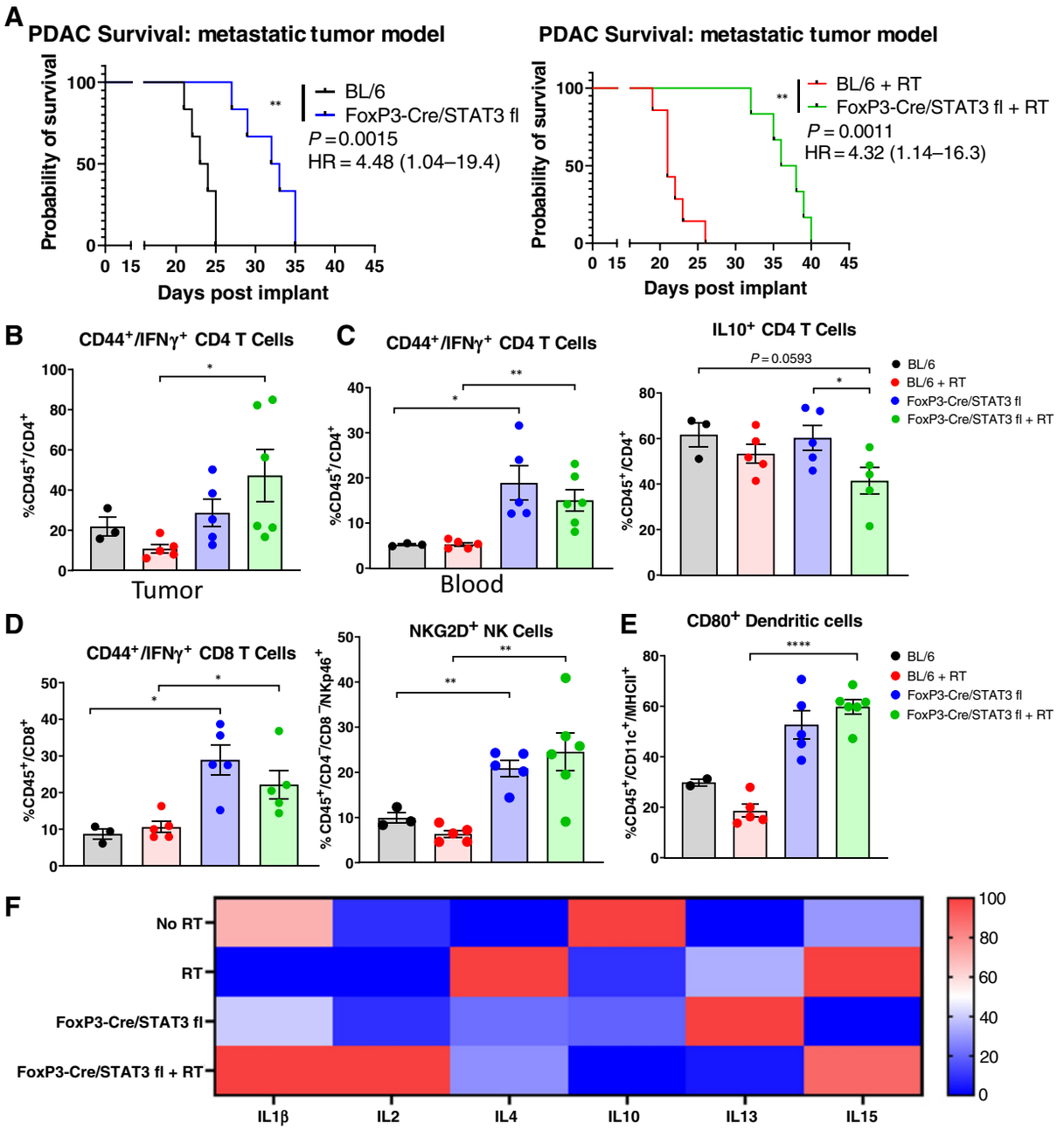

Figure 3.

Genetic targeting of STAT3 on Tregs results in improved response, enhanced activation of circulating and infiltrating immune populations. **A,** Kaplan–Meier survival analysis of WT C57BL/6 and FoxP3-Cre/STAT3 fl mice implanted with local orthotopic pancreatic tumors treated without (left) and with (right) radiotherapy (RT; $n \geq 6$ mice per group). *P* values calculated by Mantel–Cox test. **B,** Flow cytometric analysis of activated intratumoral CD4 T cells in WT C57BL/6 and FoxP3-Cre/STAT3 fl mice treated with and without RT. Activation defined as CD44/IFNγ copositivity. **C,** Analysis of circulating $CD44^+/IFN\gamma^+$ (left) and $IL10^+$ (right) CD4 T cells in tumor-bearing WT C57BL/6 and FoxP3-Cre/STAT3 fl mice treated with and without RT. **D,** Analysis of activated CD8 (left) and NK cells (right) in the circulating blood of tumor-bearing WT C57BL/6 and FoxP3-Cre/STAT3 fl mice treated with and without RT. Activation defined as CD44/IFNγ and NKG2D positivity, respectively. **E,** Flow cytometric analysis of DCs and $CD80^+$ DCs in the lymph nodes of WT C57BL/6 and FoxP3-Cre/STAT3 fl tumors treated with and without RT. DCs defined as $CD45^+/CD11c^+/MHCII^+$ cells ($n \geq 3$ for all flow cytometric analyses). **F,** Mesoscale analysis of circulating chemokines in the serum of WT C57BL/6 and FoxP3-Cre/STAT3 fl tumor-bearing mice. Error bars represent SEM. *P* values calculated with Students *t* test. *, $P < 0.05$; **, $P < 0.01$; ****, $P < 0.0001$.

Targeted inhibition of Tregs enhances NK-mediated immunosurveillance of metastasis

Given our results showing increased NK-cell activation in mice lacking STAT3 on Tregs, as well as previous reports demonstrating STAT3 signaling inhibition enhances NK-cell cytotoxicity (21), we hypothesized that not only are NKs necessary for response to treatment, but that STAT3 activity on NK cells is inhibitory of their effector function. We therefore sought to determine whether

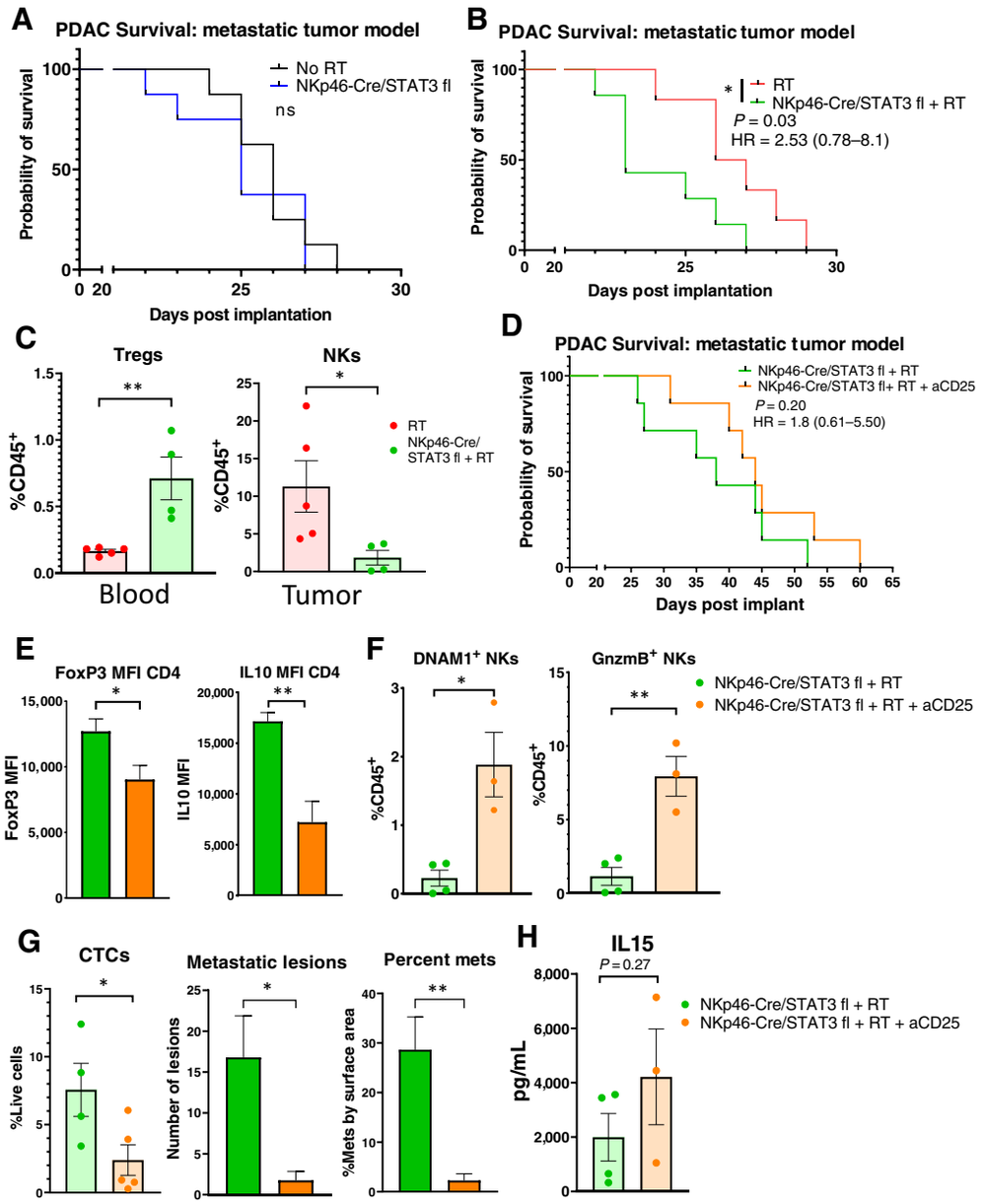

Figure 4.

Targeting Treg suppression improves NK-mediated surveillance of metastasis. Kaplan–Meier survival analysis of WT C57BL/6 and NKp46-Cre/STAT3 fl mice implanted with metastatic tumors treated without (**A**) and with (**B**) radiotherapy (RT; $n \geq 7$ mice per group). *P* values calculated by Mantel–Cox test. **C,** Frequency of circulating Tregs (left) and tumor-infiltrating NK cells (right) in WT C57BL/6 and NKp46-Cre/STAT3 fl mice implanted with orthotopic tumors ($n \geq 4$ per group). **D,** Kaplan–Meier survival analysis of tumor-bearing NKp46-Cre/STAT3 fl mice treated with RT and with or without αCD25 antibody ($n \geq 7$ mice per group). *P* values calculated by Mantel–Cox test. **E,** FoxP3 (left) and IL10 (right) MFI of tumor-infiltrating CD4 T cells in NKp46-Cre/STAT3 fl mice treated with RT and with or without αCD25 antibody ($n \geq 3$ per group). **F,** Frequency of DNAM-1$^+$ and GnzmB$^+$ intratumoral NK cells in NKp46-Cre/STAT3 fl mice treated with RT and with or without αCD25 antibody ($n \geq 3$ per group). **G,** Levels of CTCs (defined as CD45$^-$/EpCAM$^+$ cells) in the blood (left), number of metastatic lesions (center), and percent of liver exhibiting metastatic lesions by surface area (right) of NKp46-Cre/STAT3 fl mice treated with RT and with or without αCD25 antibody at time of sacrifice ($n \geq 3$ per group). **H,** Circulating IL15 levels of tumor-bearing NKp46-Cre/STAT3 fl mice treated with RT and with or without αCD25 antibody as determined by ELISA ($n \geq 3$ per group). Error bars represent SEM. *P* values calculated with Students *t* test. *, $P < 0.05$; **, $P < 0.01$; ****, $P < 0.0001$.

targeting NK-expressed STAT3 will enhance cytotoxic activity and improve response to treatment. To test this hypothesis, we used the NKp46-Cre/STAT3 fl mouse model in which STAT3 is selectively knocked out on NKp46-expressing cells. Using a metastatic tumor model, we found genetic KO of STAT3 on NKp46^{+} cells resulted in no change in survival in the absence of radiation (**Fig. 4A**; Supplementary Fig. 3C). However, STAT3 KO of NKs combined with radiotherapy significantly worsened survival over radiotherapy alone (**Fig. 4B**).

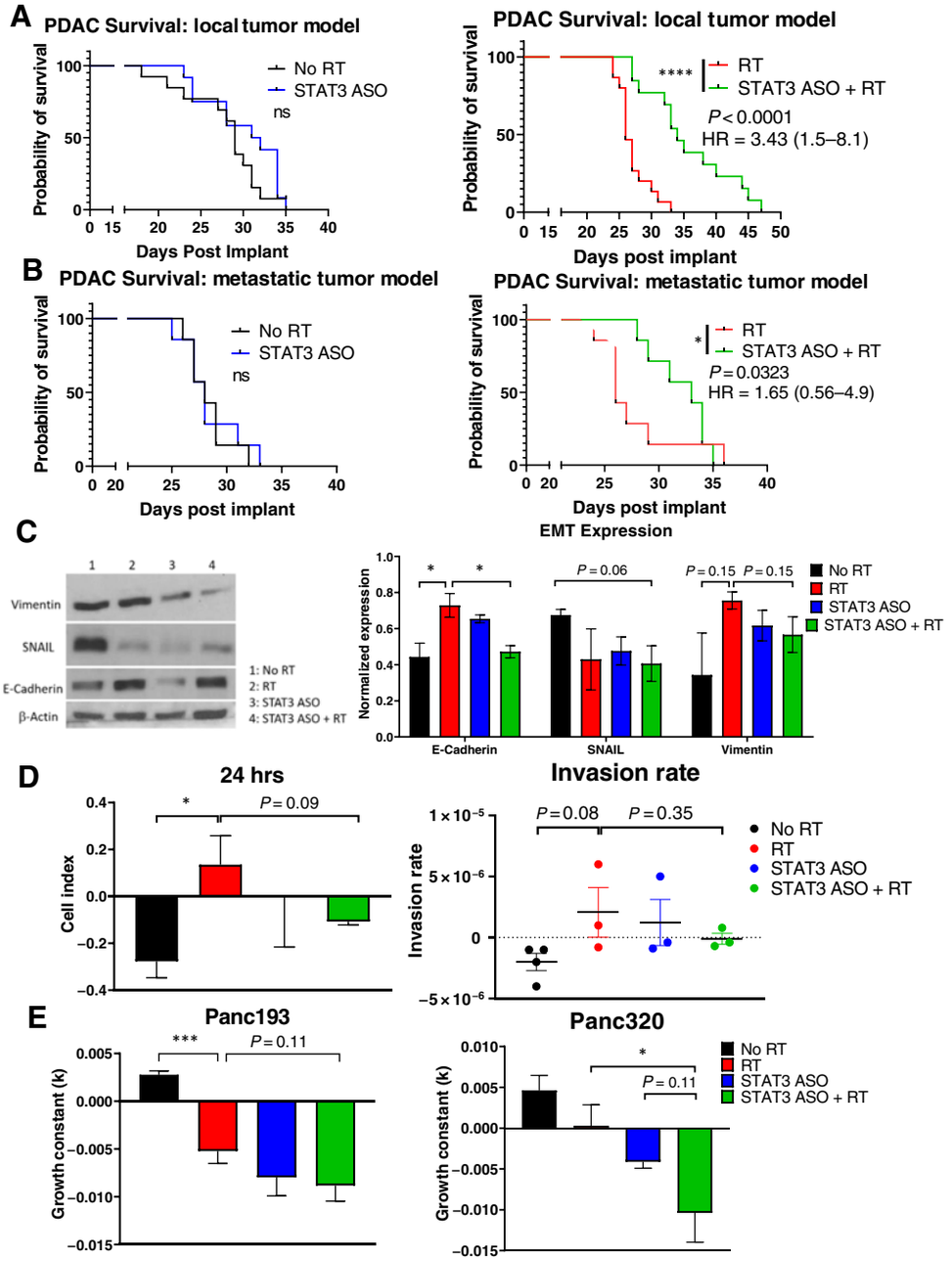

Figure 5.

STAT3 ASO + radiotherapy (RT) combination treatment results in improved survival, multicompartmental immune activation. Kaplan–Meier survival analysis of WT C57BL/6 mice bearing local orthotopic (**A**) and metastatic (**B**) tumors treated with and without STAT3 ASO and with and without RT ($n \geq 8$ mice per group). *P* values calculated by Mantel–Cox test. **C,** Western blot analysis of untreated, RT alone, STAT3 ASO alone, and STAT3 ASO + RT–treated tumors for E-cadherin, SNAIL, and vimentin (left) expression. Tumors harvested at time of sacrifice. β-Actin shown as loading control. Quantification of normalized expression (right; $n = 3$ per group). **D,** Analysis of raw invasion at 24 hours (right) and rate of invasion (left) of PK5L1940 cells treated with STAT3 ASO and RT *in vitro.* Data generated using xCELLigence RTCA equipment ($n \geq 3$ per group). **E,** Growth constant of Panc193 (left) and Panc320 (right) human organoid cell lines cocultured with human cancer associated fibroblasts. Data generated using Incyte apparatus and analyzed using Incucyte live-cell imaging analysis ($n \geq 5$ per group). (*Continued on the following page.*)

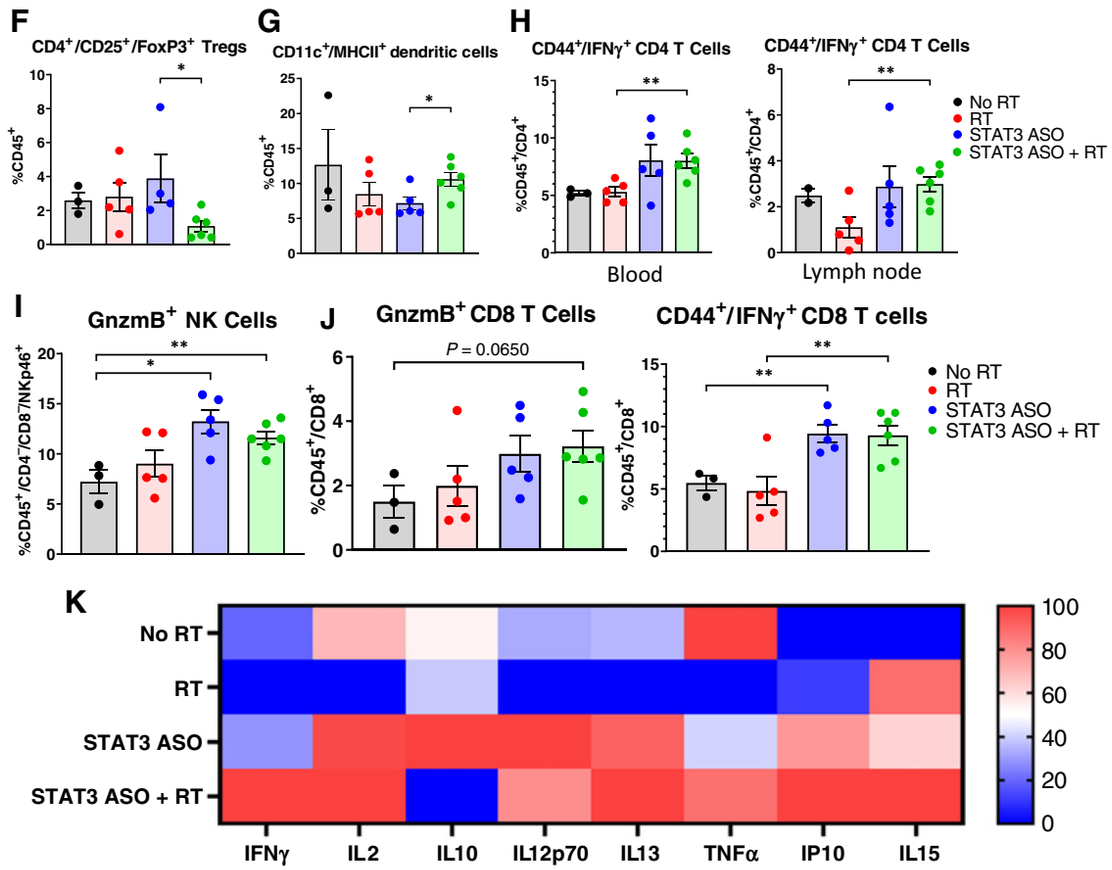

Figure 5.

(*Continued.*) Flow cytometry analysis of tumor-infiltrating regulatory T cells (**F**) and DCs (**G**) in WT C57BL/6 tumor-bearing mice treated with STAT3 ASO and RT ($n \geq 3$ per group). **H,** Flow cytometric analysis of activated CD4 T cells in the circulating blood (left) and lymph nodes (right) of WT C57BL/6 tumor-bearing mice following STAT3 ASO and RT treatment ($n \geq 3$ per group). Activation defined as CD44/IFNg copositivity. **I,** Analysis of GnzmB$^+$ NK cells in the circulating blood of STAT3 ASO and RT–treated WT C57BL/6 tumor-bearing mice ($n \geq 3$ per group). **J,** Analysis CD8 T-cell activation in the circulating blood of STAT3 ASO and RT–treated WT C57BL/6 tumor-bearing mice as defined by GnzmB positivity (left) and as CD44/IFNγ copositivity (right; $n \geq 3$ per group). **K,** Mesoscale chemokine analysis of the serum of tumor-bearing mice treated with and without RT and with or without STAT3 ASO. Error bars represent SEM. *P* values calculated with Students *t* test. *, $P < 0.05$; **, $P < 0.01$; ***, $P < 0.001$.

As this result comes contrary to previous reports, and on the basis of our data showing enhanced NK-cell activation with Treg inhibition, we next hypothesized that NK function is being suppressed by the presence of Tregs. Using a mechanistic flow cytometry–based analysis, we began by showing that, in the context of radiotherapy, NKp46-Cre/STAT3 fl mice have increased Tregs in the peripheral blood and decreased intratumoral NK-cell infiltration compared with their radiotherapy-treated WT counterparts (**Fig. 4C**). To then test the hypothesis of Treg-mediated NK suppression, we selectively depleted Tregs using an αCD25 antibody in our NKp46-Cre/STAT3 fl mouse model. While pharmacologic depletion of Tregs resulted in only a marginally improved survival and response to radiotherapy (**Fig. 4D**), αCD25 treatment resulted in significantly reduced FoxP3 and IL10 expression by tumor-infiltrating CD4 T cells, as well as an increase in intratumoral NK activation as shown by DNAM-1 and GnzmB expression (**Fig. 4E** and **F**). Of note, this increase in NK frequency and activation following αCD25 administration was less pronounced in the blood of NKp46-Cre/STAT3 fl mice relative to WT controls (Supplementary Fig. 3D–3F). Moreover, a significant reduction in CTCs, number of metastatic lesions, and the percentage of the liver displaying metastatic lesions was observed in NKp46-Cre/STAT3 fl mice treated with radiotherapy and αCD25 over radiotherapy alone (**Fig. 4G**). To validate the claim of increased activation of NK cells in NKp46-Cre/STAT3 fl mice treated with αCD25, we performed an IL15 ELISA on the serum of tumor-bearing mice and saw a trend toward an increase in IL15 in the serum of NKp46-Cre/STAT3 fl mice treated with αCD25 (**Fig. 4H**). Taken together, these data are illustrative of an important role for STAT3 in NK-mediated control of metastasis and disease spread, and are suggestive of a mechanism of Treg-induced suppression of NK cells.

Combination treatment of STAT3 ASO and radiotherapy confers survival advantage in orthotopic and metastatic tumor models

As STAT3 activity has been linked to protumorigenic effects in both immune populations and tumor cells, and given our data showing enhanced response to radiotherapy following STAT3 KO on Tregs, we hypothesized that administration of a STAT3 inhibitor would confer an improved survival advantage in our PDAC tumor

models. To test this hypothesis, mice were orthotopically implanted with PK5L1940 PDAC tumors and treated with a STAT3 ASO in the presence and absence of radiotherapy. Animals were then monitored to a survival endpoint. Using a local orthotopic tumor model, we found an improved survival advantage over control (MS = 29 days) when STAT3 ASO treatment was combined with radiotherapy (MS = 34 days; **Fig. 5A**). There was no improvement in survival, however, when mice were treated with radiotherapy (MS = 26 days) or STAT3 ASO alone (MS = 31 days), suggesting a synergistic effect for STAT3 ASO + radiotherapy treatment (**Fig. 5A**). This effect was also observed in the FC1242 KRAS–driven cell line (Supplementary Fig. 4A).

We then sought to determine the effect STAT3 ASO + radiotherapy combination treatment has on disease progression and metastatic potential of PDAC tumor cells. Using a metastatic orthotopic tumor model, we again found that survival was only improved when mice were treated with STAT3 ASO and radiotherapy (MS = 33 days; **Fig. 5B**). STAT3 ASO treatment alone (MS = 28 days) did not improve survival over control (MS = 28 days) or radiotherapy alone (MS = 26 days), suggesting combination treatment is not only effective in controlling local progression, but also distant spread. Further, STAT3 ASO + radiotherapy treatment resulted in a decrease in the expression of the epithelial–mesenchymal transition (EMT) markers vimentin, SNAIL, and E-Cadherin over control, suggesting a polarization towards a more epithelial-like and less invasive cancer cell phenotype in the combination-treated group. (**Fig. 5C**).

Of note, we also generated a CRISPR-Cas9 KO of STAT3 in our PK5L1940 cell line and implanted these cells orthotopically into the pancreas of WT mice to determine the effect of direct antitumor activity following STAT3 inhibition of cancer cells *in vivo*. We found that, without radiation, STAT3 KO significantly improves survival over WT control (MS = 34.5 vs. 26 days). However, treatment of STAT3 KO tumors with radiotherapy did not improve survival over STAT3 KO alone (Supplementary Fig. 4B), suggesting a significant contribution of immune populations to the response of STAT3 ASO + radiotherapy treatment.

Having observed a reduction in metastasis with STAT3 ASO + radiotherapy treatment *in vivo*, we next sought to examine the invasive potential of STAT3 ASO + radiotherapy–treated tumor cells *in vitro*. Using real-time cell analysis, we found that radiotherapy significantly increased the number of invading PK5L1940 cells at 24 hours over untreated control (**Fig. 5D**). However, STAT3 ASO + radiotherapy treatment resulted in fewer invading cells and a reduced rate of invasion over radiotherapy alone (**Fig. 5D**). Further, using the Panc193 and Panc320 patient-derived organoid cell lines cocultured with human stroma, we found that STAT3 ASO + radiotherapy treatment resulted in a trend toward reduced organoid growth in the Panc193 cell line and a significantly reduced organoid growth in the Panc320 cell line over radiotherapy alone. The combination-treated group also resulted in the lowest relative growth rate in both instances (**Fig. 5E**). Taken together, these data suggest that while STAT3 ASO and radiotherapy are insufficient in eliciting an improved response when administered as single agents, STAT3 ASO + radiotherapy is an effective therapy in delaying local and distant disease progression.

STAT3 ASO + radiotherapy treatment results in intratumoral and systemic immune activation

Having identified STAT3 ASO + radiotherapy as an effective treatment, we next sought to understand the mechanisms of this improved response. Using a flow cytometric analysis, we analyzed leukocyte frequency and activation in the tumor, peripheral blood, and lymph nodes of pancreatic tumor–bearing mice. This analysis showed both a significant decrease in intratumoral Tregs following STAT3 ASO + radiotherapy treatment (**Fig. 5F**), and a significant increase in tumor-infiltrating DCs in the combination group over STAT3 ASO alone (**Fig. 5G**). CD4 T-cell activation was increased in both the blood and lymph node of STAT3 ASO + radiotherapy combination–treated mice over radiotherapy alone (**Fig. 5H**). In addition, circulating NK and CD8 T cells had increased expression of activation markers including GnzmB, CD44, and IFNγ in the combination group over control (**Fig. 5I** and **J**), suggesting STAT3 ASO + radiotherapy treatment functions to increase the activity of circulating antitumor immune populations and decrease the frequency of immunosuppressive populations within the tumor.

We then analyzed the circulating cytokines present in the serum of tumor-bearing mice and found increases in the immunostimulatory cytokines IFNγ, IL2, IL12, TNFα, and, importantly, IL15, as well as a decrease in the immunosuppressive cytokine IL10 in the STAT3 ASO + radiotherapy group over control (**Fig. 5K**). Collectively, these data are suggestive of a mechanism by which STAT3 ASO + radiotherapy treatment results in sustained systemic immune activation and decreased intratumoral immunosuppression.

The improved response to radiotherapy following STAT3 inhibition is dependent on the presence of DCs and NK cells

To understand the dependency of DCs on the improved response to radiotherapy following STAT3 ASO treatment, we used the Batf3$^{-/-}$ mouse model wherein CD8a^{+} DCs, the subset responsible for CD8 T-cell cross-presentation (25), is genetically knocked out. Using this model, we found that DC depletion resulted in a significantly worsened survival (MS = 20 days) over radiotherapy alone (MS = 26 days). Further, the addition of STAT3 ASO to radiotherapy in the absence of DCs did not improve response (MS = 23 days; **Fig. 6A**). This reduction in survival was accompanied by immune modulation in various tissue compartments. In Batf3$^{-/-}$ mice treated with radiotherapy, we observed significantly reduced intratumoral CD4 and CD8 T cells compared with radiotherapy-treated WT controls (**Fig. 6B**). In the draining lymph node, DC KO resulted in a decrease in total CD4 T cells and a significantly increased presence of Tregs, suggesting that not only are there fewer nodal CD4 T cells, but the remaining CD4 T cells are more frequently Tregs, providing a possible mechanism for the worsened response to STAT3 ASO + radiotherapy treatment in the absence of CD8a^{+} DCs (**Fig. 6C**). Moreover, the absence of CD8a^{+} DCs also resulted in a decreased frequency of circulating cytotoxic populations including CD8 T cells and NK cells (**Fig. 6D**). Together, these data are suggestive of a mechanism wherein DC priming of effector immune populations is required to mediate response to radiotherapy, even in the presence of STAT3 signaling inhibition.

To further validate the dependence of DCs on response to radiotherapy, we then compared the effect of radiotherapy on the Karma mouse strain, wherein cDC1s can be selectively depleted (26), to the observed effect on the Batf3$^{-/-}$ strain. Using these two genetically engineered mouse models, we found a significant increase in tumor growth in the Batf3$^{-/-}$ strain over the Karma strain (**Fig. 6E**), which was correlated with a decrease in CD103 expression of intratumoral DCs (**Fig. 6F**). These findings suggest a critical role for intratumoral CD103^{+} DCs in delaying tumor growth and promoting an antitumor immune response following radiotherapy.

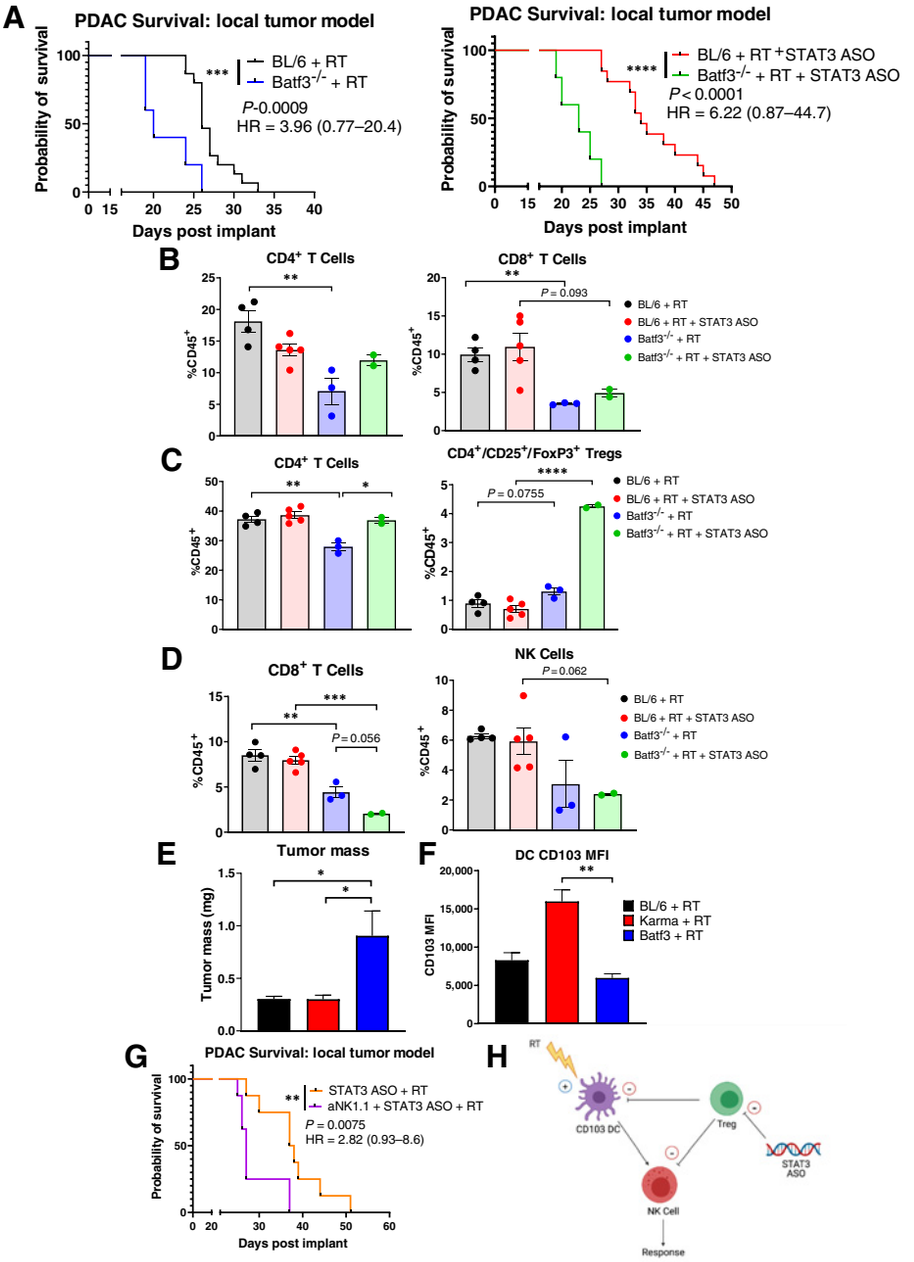

Figure 6.

DC presence is required for response to STAT3 ASO + radiotherapy (RT) combination therapy. **A,** Kaplan–Meier survival analysis of WT C57BL/6 and Batf3$^{-/-}$ mice implanted with local orthotopic pancreatic tumors ($n \geq 7$ mice per group). *P* values calculated by Mantel–Cox test. **B,** Flow cytometric analysis of intratumoral CD4 (left) and CD8 (right) T cells in WT C57BL/6 and Batf3$^{-/-}$ mice treated with and without RT ($n \geq 2$ per group). **C,** CD4 (left) and Treg (right) frequency in lymph nodes of WT C57BL/6 and Batf3$^{-/-}$ tumor-bearing mice as determined by flow cytometry ($n \geq 2$ per group). **D,** Analysis of CD8 T cells (left) and NK cells (right) in the circulating blood of WT C57BL/6 and Batf3$^{-/-}$ tumor-bearing mice treated with and without RT ($n \geq 2$ per group). **E,** Tumor mass quantification of tumors harvested from WT C57BL/6, Batf3$^{-/-}$, and Karma mice at day 21 post-implantation ($n \geq 3$ per group). **F,** CD103 MFI of intratumoral DCs in WT C57BL/6, Batf3$^{-/-}$, and Karma DTR mice as determined by flow cytometry ($n \geq 3$ per group). *P* values calculated with Students *t* test. Error bars represent SEM. **G,** Kaplan–Meier survival analysis of WT C57BL/6 mice treated with STAT3 ASO + RT and with or without αNK1.1 NK-cell–depleting antibody ($n \geq 6$ mice per group). *P* values calculated by Mantel–Cox test. *, $P < 0.05$; **, $P < 0.01$; ***, $P < 0.001$; ****, $P < 0.0001$. **H,** Model of interactions between immune populations.

To further elucidate the signaling mechanisms of STAT3 ASO + radiotherapy treatment and to corroborate our patient sequencing data highlighting the importance of intratumoral NK cells in response to treatment in PDAC, we next sought to understand the dependence of NK cell activity on the improved response to STAT3 ASO + radiotherapy treatment. Through antibody-mediated depletion, we found that the beneficial effect of STAT3 ASO + radiotherapy combination treatment is abrogated in the absence of NK cells (**Fig. 6G**), suggesting a critical role for NKs in mediating an antitumor immune response. Using a flow cytometric analysis, we found that the diminished response to STAT3 ASO + radiotherapy treatment following NK depletion was accompanied by an increase in IL10 and FoxP3 expression by CD4 T cells in the tumor (Supplementary Fig. 5A), as well as a decrease in CD103 expression by DCs and CD4 T-cell activation in the lymph node (Supplementary Fig. 5B). A schematic of the proposed cellular interactions is provided in **Fig. 6H**.

Discussion

Resistance to treatment remains a major hurdle to overcome in pancreatic cancer. In this study, we investigated the role of STAT3 signaling in Tregs and the resulting effect that Treg-expressed STAT3 has on systemic immunosuppression and disease progression.

Although targeting cellular and molecular mediators of treatment failure, such as STAT3 (27–29), have shown promise as effective therapies, these strategies seem to have ambiguous and sometimes even antagonistic effects on cellular subsets in the complex TME of PDAC (30, 31). As cancer cell–expressed STAT3 has been implicated in a variety of protumorigenic pathways, the STAT3 signaling cascade has become the target of novel chemotherapeutic agents (32–34). However, the effect of STAT3 inhibition on other cellular compartments in the TME is less understood. Here, we sought to explore the role of STAT3 activity in Tregs and NK cells and examine how this signaling relates to the antitumor immune response following radiotherapy. We show that STAT3 signaling inhibition can be used to combat immunosuppression and maintain the transient immunostimulatory effects of radiotherapy, an effect that results in enhanced activation of effector immune populations and improved survival.

A key finding of our research is that Tregs are a core element of therapeutic resistance in pancreatic cancer, and it is only with their inhibition that both local and systemic control is established. Although the presence and frequency of intratumoral Tregs has been correlated with poor prognosis in pancreatic cancer, depletion of this cell type has been met with varying responses (35, 36). Using genetic and pharmacologic manipulation, we found that the response to radiotherapy is only enhanced when Tregs are either depleted or are the target of functional inhibition. In targeting the functional capacity of Tregs, we found that mice with a genetic deficiency of STAT3 in the Treg compartment have diminished systemic immunosuppression and improved survival following radiotherapy treatment. Of critical importance, we show that targeting Treg function results in a significant reduction in the presence of CTCs and a diminished metastatic burden. Also, only in the absence of Tregs does genetic targeting of STAT3 on NKp46$^+$ cells result in enhanced immunosurveillance and improved response, providing additional evidence to support the notion that Tregs are the master regulators of resistance to therapy and response is only improved in a system devoid of Treg-induced immunosuppression.

The central role NKs play in controlling metastatic progression (37–39), and as supported by our data, is therapeutically provocative as it suggests agonistic therapies aimed at activating NKs may have meaningful clinical relevance, but only when Treg function is inhibited. Here, we not only show that the therapeutic effect of STAT3 ASO + radiotherapy combination treatment is dependent on the presence of NK cells, but we also found that in the absence of NKs, the incidence and severity of metastatic spread is significantly increased. As NKs have been correlated with improved overall survival in PDAC and as there is growing evidence for a role for NKs in eliciting an antitumor immune response, these findings suggest maintaining activation may enhance NK-mediated surveillance of CTCs and improve response to radiotherapy. However, the data presented here suggest that while agents aimed at agonizing NKs have the potential to be therapeutically effective, they are insufficient if administered alone without also targeting Treg-mediated immunosuppression.

Finally, the controversial role for radiotherapy cannot be overlooked given the recent results of the ALLIANCE trial (9), begging the question of whether radiotherapy is required in the context of immune stimulation. The data presented here are supportive of an immunostimulatory role for radiotherapy as we show that radiotherapy increases DC activation and CD103 expression, enhancing response to STAT3 ASO + radiotherapy treatment (40–42). Moreover, we show that radiotherapy-induced activation of DCs is critical to response as in the absence of these activated DC subsets, the therapeutic efficacy of STAT3 ASO + radiotherapy combination treatment is abrogated. Using mouse models with genetic KO of varying DC subsets, we found that the Batf3$^{-/-}$ mouse strain lacking CD103$^+$ DCs does not respond to STAT3 ASO + radiotherapy combination treatment, while the Karma DTR mouse strain devoid of XCR1$^+$ DCs maintains a baseline response, suggestive of a critical role for the CD103$^+$ population of DCs in mediating response to treatment. However, despite their critical role in response to treatment, radiotherapy-mediated activation of DCs may be insufficient in maintaining systemic IL15 levels. Here, we show cancer cell–expressed IL15 to be a contributor to IL15 production in PDAC (Supplementary Fig. 5C), suggesting radiotherapy-induced cancer cell death may lead to a net decrease in IL15 levels in a DC-independent manner.

Of particular importance, while the development of small molecule STAT3 inhibitors have been met with challenges due to drug-related toxicities including thrombocytopenia, neuropathies, and pneumonitis (43), the STAT3 ASO employed in the present study has been shown to be well tolerated in patients (44).

In summary, our data identify Tregs as a critical target of inhibition to enhance DC and NK-cell activation and not only invigorate T-cell effector function within the TME, but also improve immunosurveillance of metastatic spread by activated NK cells in circulation. These results identify combination therapies such as STAT3 ASO with radiotherapy in improving response to treatment in pancreatic cancer.

Authors' Disclosures

A. Mueller reports grants from Radiological Society of North America during the conduct of the study. A. Dent reports grants from NIH/NIAID during the conduct of the study. M. Del Chiaro reports other support from Boston Scientific and grants from Haemonetics, Inc outside the submitted work. L. Lenz reports grants from NIH during the conduct of the study, as well as grants from NIH outside the submitted work; in addition, L. Lenz has a patent for PCT/US2010056266 issued to National Jewish Health, and has served on scientific advisory boards for Brenzole, LLC and Bebra Therapeutics, LLC. S.D. Karam reports grants from AstraZeneca during the conduct of the study, as well as grants from AstraZeneca, Genentech, and Roche outside the submitted work. No disclosures were reported by the other authors.

Authors' Contributions

M. Piper: Conceptualization, data curation, formal analysis, supervision, investigation, visualization, writing–original draft, writing–review and editing. **B. Van Court:** Conceptualization, data curation, formal analysis, visualization, writing–review and editing. **A. Mueller:** Conceptualization, data curation, writing–review and editing. **S. Watanabe:** Data curation, writing–review and editing. **T. Bickett:** Conceptualization, writing–review and editing. **S. Bhatia:** Conceptualization, writing–review and editing. **L.B. Darragh:** Conceptualization, writing–review and editing. **M. Mayeda:** Data curation. **D. Nguyen:** Data curation, writing–review and editing. **J. Gadwa:** Writing–review and editing. **M. Knitz:** Writing–review and editing. **S. Corbo:** Writing–review and editing. **R. Morgan:** Resources, methodology, writing–review and editing. **J.-J. Lee:** Conceptualization, investigation, writing–review and editing. **A. Dent:** Resources, writing–review and editing. **K. Goodman:** Resources, supervision, investigation, writing–review and editing. **W. Messersmith:** Resources, investigation, writing–review and editing. **R. Schulick:** Resources, investigation, methodology, writing–review and editing. **M. Del Chiaro:** Resources, investigation, methodology, writing–review and editing. **Y. Zhu:** Resources, validation, writing–review and editing. **R.M. Kedl:** Resources, validation, writing–review and editing. **L. Lenz:** Resources, validation, writing–review and editing. **S.D. Karam:** Conceptualization, resources, supervision, funding acquisition, investigation, writing–original draft, project administration, writing–review and editing.

Acknowledgments

This work is supported by the National Institute of Dental and Craniofacial Research (to SDK, 1 P50 CA261605–01, R01 DE028529–01, R01 DE028282–01), the Wings of Hope Pancreatic Cancer Research Funding grant, and the Cancer League of Colorado. The authors would like to thank Dr. Edward Chan (National Jewish Health, Denver, CO) for providing DEREG mice. The authors would also like to acknowledge Ionis Pharmaceuticals (Carlsbad, CA) for providing the STAT3 ASO. We thank the University of Colorado Cancer Center Genomics and Microarray Shared Resource, Human Immune Monitoring Shared Resource, Functional Genomics Shared Resource, Small Animal Irradiation Core, Animal Imaging Shared Resource, Biostatistics and Bioinformatics Shared Resource, Protein Production/Monoclonal Antibody/Tissue Culture Shared Resource, and Flow Cytometry Shared Resource, each supported in part by the Cancer Center Support Grant (P30CA046934). Some of the imaging experiments were performed in the Advanced Light Microscopy Core, part of the NeuroTechnology Center at the University of Colorado Anschutz Medical Campus, supported in part by Rocky Mountain Neurological Disorders Core Grant Number P30 NS048154 and by Diabetes Research Center Grant Number P30 DK116073.

The costs of publication of this article were defrayed in part by the payment of page charges. This article must therefore be hereby marked *advertisement* in accordance with 18 U.S.C. Section 1734 solely to indicate this fact.

Received July 30, 2021; revised October 1, 2021; accepted November 29, 2021; published first December 2, 2021.

References

1. Siegel RL, Miller KD, Jemal A. Cancer statistics, 2020. CA Cancer J Clin 2020;70:7–30.
2. Oweira H, Petrausch U, Helbling D, Schmidt J, Mannhart M, Mehrabi A, et al. Prognostic value of site-specific metastases in pancreatic adenocarcinoma: a surveillance epidemiology and end results database analysis. World J Gastroenterol 2017;23:1872–80.
3. Quail DF, Joyce JA. Microenvironmental regulation of tumor progression and metastasis. Nat Med 2013;19:1423–37.
4. Sahin IH, Elias H, Chou JF, Capanu M, O'Reilly EM. Pancreatic adenocarcinoma: insights into patterns of recurrence and disease behavior. BMC Cancer 2018;18:769.
5. Amedei A, Niccolai E, Benagiano M, Della Bella C, Cianchi F, Bechi P, et al. Ex vivo analysis of pancreatic cancer-infiltrating T lymphocytes reveals that ENO-specific Tregs accumulate in tumor tissue and inhibit Th1/Th17 effector cell functions. Cancer Immunol Immunother 2013;62:1249–60.
6. Ino Y, Yamazaki-Itoh R, Shimada K, Iwasaki M, Kosuge T, Kanai Y, et al. Immune cell infiltration as an indicator of the immune microenvironment of pancreatic cancer. Br J Cancer 2013;108:914–23.
7. Liyanage UK, Moore TT, Joo HG, Tanaka Y, Herrmann V, Doherty G, et al. Prevalence of regulatory T cells is increased in peripheral blood and tumor microenvironment of patients with pancreas or breast adenocarcinoma. J Immunol 2002;169:2756–61.
8. Zhao F, Obermann S, von Wasielewski R, Haile L, Manns MP, Korangy F, et al. Increase in frequency of myeloid-derived suppressor cells in mice with spontaneous pancreatic carcinoma. Immunology 2009;128:141–9.
9. Katz MHG, Shi Q, Meyers JP, Herman JM, Choung M, Wolpin BM, et al. Alliance A021501: preoperative mFOLFIRINOX or mFOLFIRINOX plus hypofractionated radiation therapy (RT) for borderline resectable (BR) adenocarcinoma of the pancreas. J Clin Oncol 2021;39:377.
10. Reyngold M, O'Reilly EM, Varghese AM, Fiasconaro M, Zinovoy M, Romesser PB, et al. Association of ablative radiation therapy with survival among patients with inoperable pancreatic cancer. JAMA Oncol 2021;7:735–38.
11. Cellini F, Arcelli A, Simoni N, Caravatta L, Buwenge M, Calabrese A, et al. Basics and frontiers on pancreatic cancer for radiation oncology: target delineation, SBRT, SIB technique, MRgRT, particle therapy, immunotherapy, and clinical guidelines. Cancers (Basel) 2020;12:1729.
12. Lesina M, Kurkowski MU, Ludes K, Rose-John S, Treiber M, Klöppel G, et al. Stat3/Socs3 activation by IL-6 transsignaling promotes progression of pancreatic intraepithelial neoplasia and development of pancreatic cancer. Cancer Cell 2011;19:456–69.
13. Jiang H, Liu X, Knolhoff BL, Hegde S, Lee KB, Jiang H, et al. Development of resistance to FAK inhibition in pancreatic cancer is linked to stromal depletion. Gut 2020;69:122–32.
14. Wu X, Tang W, Marquez RT, Li K, Highfill CA, He F, et al. Overcoming chemo/radio-resistance of pancreatic cancer by inhibiting STAT3 signaling. Oncotarget 2016;7:11708–23.
15. Aran D, Hu Z, Butte AJ. xCell: digitally portraying the tissue cellular heterogeneity landscape. Genome Biol 2017;18:220.
16. Qiu W, Su GH. Development of orthotopic pancreatic tumor mouse models. Methods Mol Biol 2013;980:215–23.
17. Soares KC, Foley K, Olino K, Leubner A, Mayo SC, Jain A, et al. A preclinical murine model of hepatic metastases. J Vis Exp 2014;51677.
18. Ali AK, Nandagopal N, Lee SH. IL-15-PI3K-AKT-mTOR: a critical pathway in the life journey of natural killer cells. Front Immunol 2015;6:355.
19. Oweida AJ, Mueller AC, Piper M, Milner D, Van Court B, Bhatia S, et al. Response to radiotherapy in pancreatic ductal adenocarcinoma is enhanced by inhibition of myeloid-derived suppressor cells using STAT3 antisense oligonucleotide. Cancer Immunol Immunother 2020;70:989–1000.
20. Hossain DM, Panda AK, Manna A, Mohanty S, Bhattacharjee P, Bhattacharyya S, et al. FoxP3 acts as a cotranscription factor with STAT3 in tumor-induced regulatory T cells. Immunity 2013;39:1057–69.
21. Gotthardt D, Putz EM, Straka E, Kudweis P, Biaggio M, Poli V, et al. Loss of STAT3 in murine NK cells enhances NK-cell–dependent tumor surveillance. Blood 2014;124:2370–9.
22. Lahl K, Sparwasser T. *In vivo* depletion of FoxP3$^+$ Tregs using the DEREG mouse model. Methods Mol Biol 2011;707:157–72.
23. Mueller AC, Piper M, Goodspeed A, Bhuvane S, Williams JS, Bhatia S, et al. Induction of ADAM10 by RT drives fibrosis, resistance, and EMT in pancreatic cancer. Cancer Res 2021;81:3255–69.
24. Zorn E, Nelson EA, Mohseni M, Porcheray F, Kim H, Litsa D, et al. IL-2 regulates FOXP3 expression in human CD4$^+$CD25$^+$ regulatory T cells through a STAT-dependent mechanism and induces the expansion of these cells *in vivo*. Blood 2006;108:1571–9.
25. Chen L, Zhang D, Zhang W, Zhu Y, Hou M, Yang B, et al. Absence of Batf3 results in reduced liver pathology in mice infected with *Schistosoma japonicum*. Parasit Vectors 2017;10:306.
26. Mattiuz R, Wohn C, Ghilas S, Ambrosini M, Alexandre YO, Sanchez C, et al. Novel Cre-expressing mouse strains permitting to selectively track and edit Type 1 conventional dendritic cells facilitate disentangling their complexity *in vivo*. Front Immunol 2018;9:2805.
27. Nagaraj NS, Washington MK, Merchant NB. Combined blockade of Src kinase and epidermal growth factor receptor with gemcitabine overcomes STAT3-mediated resistance of inhibition of pancreatic tumor growth. Clin Cancer Res 2011;17:483–93.
28. Kanda N, Seno H, Konda Y, Marusawa H, Kanai M, Nakajima T, et al. STAT3 is constitutively activated and supports cell survival in association with survivin expression in gastric cancer cells. Oncogene 2004;23:4921–9.
29. Jin W. Role of JAK/STAT3 signaling in the regulation of metastasis, the transition of cancer stem cells, and chemoresistance of cancer by epithelial–mesenchymal transition. Cells 2020;9:217.
30. Hillmer EJ, Zhang H, Li HS, Watowich SS. STAT3 signaling in immunity. Cytokine Growth Factor Rev 2016;31:1–15.
31. Yu H, Kortylewski M, Pardoll D. Crosstalk between cancer and immune cells: role of STAT3 in the tumor microenvironment. Nat Rev Immunol 2007;7:41–51.
32. Sau S, Mondal SK, Kashaw SK, Iyer AK, Banerjee R. Combination of cationic dexamethasone derivative and STAT3 inhibitor (WP1066) for aggressive melanoma: a strategy for repurposing a phase I clinical trial drug. Mol Cell Biochem 2017;436:119–36.
33. Mukthavaram R, Ouyang X, Saklecha R, Jiang P, Nomura N, Pingle SC, et al. Effect of the JAK2/STAT3 inhibitor SAR317461 on human glioblastoma tumorspheres. J Transl Med 2015;13:269.
34. Han D, Yu T, Dong N, Wang B, Sun F, Jiang D. Napabucasin, a novel STAT3 inhibitor suppresses proliferation, invasion, and stemness of glioblastoma cells. J Exp Clin Cancer Res 2019;38:289.
35. Zhang Y, Lazarus J, Steele NG, Yan W, Lee HJ, Nwosu ZC, et al. Regulatory T-cell depletion alters the tumor microenvironment and accelerates pancreatic carcinogenesis. Cancer Discov 2020;10:422–39.

36. Jang JE, Hajdu CH, Liot C, Miller G, Dustin ML, Bar-Sagi D. Crosstalk between regulatory T cells and tumor-associated dendritic cells negates antitumor immunity in pancreatic cancer. Cell Rep 2017;20:558–71.
37. López-Soto A, Gonzalez S, Smyth MJ, Galluzzi L. Control of metastasis by NK cells. Cancer Cell 2017;32:135–54.
38. Krasnova Y, Putz EM, Smyth MJ, Souza-Fonseca-Guimaraes F. Bench to bedside: NK cells and control of metastasis. Clin Immunol 2017;177:50–59.
39. Lorenzo-Herrero S, López-Soto A, Sordo-Bahamonde C, Gonzalez-Rodriguez AP, Vitale M, Gonzalez S. NK-cell–based immunotherapy in cancer metastasis. Cancers 2018;11:29.
40. Hegde S, Krisnawan VE, Herzog BH, Zuo C, Breden MA, Knolhoff BL, et al. Dendritic cell paucity leads to dysfunctional immune surveillance in pancreatic cancer. Cancer Cell 2020;37:289–307.e9.
41. Wylie B, Macri C, Mintern JD, Waithman J. Dendritic cells and cancer: from biology to therapeutic intervention. Cancers 2019;11:521.
42. Yang J, Shangguan J, Eresen A, Li Y, Wang J, Zhang Z. Dendritic cells in pancreatic cancer immunotherapy: vaccines and combination immunotherapies. Pathol Res Pract 2019;215:152691.
43. Proia TA, Singh M, Woessner R, Carnevalli L, Bommakanti G, Magiera L, et al. STAT3 antisense oligonucleotide remodels the suppressive tumor microenvironment to enhance immune activation in combination with anti–PD-L1. Clin Cancer Res 2020;26:6335–49.
44. Reilley MJ, McCoon P, Cook C, Lyne P, Kurzrock R, Kim Y, et al. STAT3 antisense oligonucleotide AZD9150 in a subset of patients with heavily pretreated lymphoma: results of a phase Ib trial. J Immunother Cancer 2018;6:119.